



**HAL**  
open science

## Repeated Autologous Bone Marrow-Derived Mesenchymal Stem Cell Injections Improve Radiation-Induced Proctitis in Pigs

Christine Linard, Elodie Busson, Valérie Holler, Carine Strup-Perrot,  
Jean-Victor Lacave-Lapalun, Bruno Lhomme, Marie Prat, Patrick  
Devauchelle, Jean-Christophe Sabourin, Jean-Marc Simon, et al.

### ► To cite this version:

Christine Linard, Elodie Busson, Valérie Holler, Carine Strup-Perrot, Jean-Victor Lacave-Lapalun, et al.. Repeated Autologous Bone Marrow-Derived Mesenchymal Stem Cell Injections Improve Radiation-Induced Proctitis in Pigs. *Stem Cells Translational Medicine*, 2013, 2 (11), pp.916 - 927. 10.5966/sctm.2013-0030 . hal-02647101

**HAL Id: hal-02647101**

**<https://hal.inrae.fr/hal-02647101>**

Submitted on 29 May 2020

**HAL** is a multi-disciplinary open access archive for the deposit and dissemination of scientific research documents, whether they are published or not. The documents may come from teaching and research institutions in France or abroad, or from public or private research centers.

L'archive ouverte pluridisciplinaire **HAL**, est destinée au dépôt et à la diffusion de documents scientifiques de niveau recherche, publiés ou non, émanant des établissements d'enseignement et de recherche français ou étrangers, des laboratoires publics ou privés.

Copyright



## Repeated Autologous Bone Marrow-Derived Mesenchymal Stem Cell Injections Improve Radiation-Induced Proctitis in Pigs

CHRISTINE LINARD,<sup>a</sup> ELODIE BUSSON,<sup>b</sup> VALERIE HOLLER,<sup>a</sup> CARINE STRUP-PERROT,<sup>a</sup> JEAN-VICTOR LACAVER-LAPALUN,<sup>a</sup> BRUNO LHOMME,<sup>a</sup> MARIE PRAT,<sup>b</sup> PATRICK DEVAUCHELLE,<sup>c</sup> JEAN-CHRISTOPHE SABOURIN,<sup>d</sup> JEAN-MARC SIMON,<sup>e</sup> MICHEL BONNEAU,<sup>f</sup> JEAN-JACQUES LATAILLADE,<sup>b</sup> MARC BENDERITTER<sup>a</sup>

**Key Words.** Mesenchymal stem cells • Irradiation • Pig model • Cellular therapy

### ABSTRACT

The management of proctitis in patients who have undergone very-high-dose conformal radiotherapy is extremely challenging. The fibrosis-necrosis, fistulae, and hemorrhage induced by pelvic overirradiation have an impact on morbidity. Augmenting tissue repair by the use of mesenchymal stem cells (MSCs) may be an important advance in treating radiation-induced toxicity. Using a preclinical pig model, we investigated the effect of autologous bone marrow-derived MSCs on high-dose radiation-induced proctitis. Irradiated pigs received repeated intravenous administrations of autologous bone marrow-derived MSCs. Immunostaining and real-time polymerase chain reaction analysis were used to assess the MSCs' effect on inflammation, extracellular matrix remodeling, and angiogenesis, in radiation-induced anorectal and colon damages. In humans, as in pigs, rectal overexposure induces mucosal damage (crypt depletion, macrophage infiltration, and fibrosis). In a pig model, repeated administrations of MSCs controlled systemic inflammation, reduced *in situ* both expression of inflammatory cytokines and macrophage recruitment, and augmented interleukin-10 expression in rectal mucosa. MSC injections limited radiation-induced fibrosis by reducing collagen deposition and expression of col1a2/col3a1 and transforming growth factor- $\beta$ /connective tissue growth factor, and by modifying the matrix metalloproteinase/TIMP balance. In a pig model of proctitis, repeated injections of MSCs effectively reduced inflammation and fibrosis. This treatment represents a promising therapy for radiation-induced severe rectal damage. *STEM CELLS TRANSLATIONAL MEDICINE* 2013;2:916–927

### INTRODUCTION

Conformal radiotherapy in the pelvic area is associated with a high incidence of acute and/or chronic intestinal complications due to the low tolerance of organs at risk (colon, rectum, and bladder) in the radiation field. Radiation proctopathy is defined as symptomatic radiation-induced damage to the lining of the rectum that commonly occurs as a result of radiotherapy for prostate cancer. Approximately 13% of patients receiving conventional pelvic radiotherapy [1] develop acute rectal symptoms (grade II or below), which usually present initially as nonbloody diarrhea. This generally begins around 2–4 weeks into treatment and may be accompanied by tenesmus, abdominal cramps, or, rarely, bleeding. Five percent to 10% of patients develop chronic radiation proctopathy that occurs months to years after treatment but mostly within 2 years after radiation and at an average of 8–12 months [2]. An increased risk of grade II or III toxicity appears when more

than 25%–30% of the rectal wall volume receives more than 70 Gy [3]. The clinical manifestation of proctitis may involve small-volume intermittent bleeding, possibly accompanied by constipation, abdominal cramps, and mucoid discharge. Endoscopy reveals pallor, telangiectatic vessels, and friable mucosa [4]. Usually, there is evidence of vasculitis with arteriolar thrombosis, leading to ischemia and eventually to ulceration and bleeding. Patients who are severely affected may require frequent blood transfusions. Over months to years, progression to fibrosis and scarring may occur, resulting in stricture or fistula formation [5], increasing the morbidity risk [6]. In a recently reported radiation oncology accident at the Public General Hospital of Epinal, France, patients undergoing conformal radiotherapy for prostate cancer received a 20% overdosage, with 25% of the rectum receiving more than 75 Gy [6]. Grade II to IV toxicity on the Common Terminology Criteria for Adverse Events 3.0 scale has been reported as requiring

<sup>a</sup>Institute of Radiological Protection and Nuclear Safety, Fontenay-aux-Roses, France; <sup>b</sup>Research and Cell Therapy Department, Military Blood Transfusion Center, Percy Military Hospital, Clamart, France; <sup>c</sup>Centre of Radiotherapy Scanner, National Veterinary School, Maison-Alfort, France; <sup>d</sup>Department of Pathology, Rouen University Hospital, Rouen, France; <sup>e</sup>Department of Radiation Oncology, Pitie-Salpetriere University Hospital, Paris, France; <sup>f</sup>Centre of Research in Interventional Imaging, Institut National de la Recherche Agronomique, Jouy-en-Josas, France

Correspondence: Christine Linard, Ph.D., Institut de Radioprotection et de Sûreté Nucléaire, B.P. no. 17, F-92262 Fontenay-aux-Roses, France. Telephone: 33-1-58-35-91-86; Fax: 33-1-58-35-84-67; E-Mail: christine.linard@irsn.fr

Received February 21, 2013; accepted for publication June 4, 2013; first published online in *SCTM EXPRESS* September 25, 2013.

©AlphaMed Press  
1066-5099/2013/\$20.00/0

<http://dx.doi.org/10.5966/sctm.2013-0030>

a colostomy and presenting as severe pain refractory to opioid therapy. In this rectal injury, conservative treatment options including medical, coagulation, and hyperbaric oxygen therapies and surgery are of limited value.

Originally isolated from bone marrow (BM), mesenchymal stem cells (MSCs) are pluripotent progenitor cells that contribute to the maintenance and regeneration of various connective tissues [7, 8]. Therefore, MSCs are expected to become a source of cells for regenerative therapy [9, 10]. In these applications, currently undergoing phase III clinical trials, MSCs are considered not to contribute significantly by direct differentiation and replacement of the damaged tissue, but rather to perform as trophic mediators [11], promoting tissue repair by production and release of soluble factors that inhibit inflammation [12], reduce fibrosis, and induce angiogenesis [13]. Especially in intestine, previous studies showed that bone marrow-derived MSCs contribute to tissue repair by differentiation into vascular smooth muscle cells, endothelial cells, pericytes, or epithelial cells [14, 15]. Rodent models showed that MSC transplantation prevents radiation-induced intestinal injury by both increasing endogenous proliferation and inhibiting apoptosis [16, 17]. To evaluate the potential of MSC treatment for patients severely affected by a high irradiation dose, we developed a preclinical pig proctitis model. Using external-beam radiotherapy with a three-field technique, we demonstrated that autologous bone marrow-derived MSC injections reduced the inflammatory response and reduced fibrosis.

## MATERIALS AND METHODS

### Collection of Human Tissue Samples

Three patients treated for prostate cancer who were victims in the radiation oncology accident at the Public Hospital in Epinal, France, were included in this study. Post-treatment toxicities were all graded (grades III and IV) according to the Common Terminology Criteria for Adverse Events (3.0 scale). Some endoscopic anorectum biopsies coming from the EPOPA trial (Patients Overexposed for a Prostate Adenocarcinoma, ClinicalTrials.gov no. NCT00773656). This clinical study has received an approval from the French health ministry (<http://clinicaltrials.gov/show/NCT00773656>). The rectal tissues from nonirradiated areas (obtained following the ethical guidelines of the Gustave Roussy Institute and the French Medical Research Council) were fixed in neutral buffered formalin and paraffin embedded. Sections (5  $\mu$ m) were stained with hematoxylin-eosin for histologic assessment, and collagen deposition was detected by Sirius red staining. Macrophages were detected using a monoclonal mouse anti-human CD68 antibody (Dako, Trappes, France, <http://www.dako.com>). For matrix metalloproteinase-9 (MMP-9) detection, sections were pretreated with trypsin and incubated with MMP-9 antibody (NB100-78557; Novus Biologicals, Littleton, CO, <http://www.novusbio.com>). All patients gave informed written consent to this study.

### Animal Care

Male Göttingen pigs, 12 months old and weighing approximately 20–25 kg, from Ellegaard (Dalmose, Denmark, <http://www.minipigs.dk>), were placed in individual pens (21°C, 12-hour/12-hour light-dark schedule) in which they received solid food and had access to water ad libitum. All experiments were conducted

in accordance with French regulations for animal experiments (Ministry of Agriculture Order B92-032-01, 2006).

### Experimental Design

Anesthetized (1.5% isoflurane in oxygen) animals received a high x-ray dose (Dr. Devauchelle, Radiotherapy-Scanner Center, Maisons-Alfort, France) delivered in three external beams to the rectum: one anterior and two lateral beams. Physical dosimetry was evaluated using thermoluminescent dosimeters with alumina powder placed in the rectum (supplemental online Table 1). Six pigs were included in this study: three irradiated pigs with no further treatment and three irradiated pigs that received three systemic administrations of MSCs. The MSC-treated pigs were injected under anesthesia (1.5% isoflurane in oxygen) at the genesis of fibrosis previewed at the colonoscopy with autologous MSCs ( $2 \times 10^6$  MSCs per kilogram in sterile phosphate-buffered saline [PBS]) in the ear vein once a week on days 27, 34, and 41 postirradiation. Non-MSC-treated pigs were injected with PBS alone according to the same scheme.

### Porcine Clinical Follow-Up

During the follow-up period, minipigs were examined clinically every day, and blood samples were collected twice a week. Stool condition was scored: grade 0, normal to semisolid stools, no blood; grade 1, normal to semisolid stools; grade 2: semisolid to fluid stools, blood-tinged; grade 3, fluid, presence of blood. Endoscopies were carried out on anesthetized animals at day 15 and day 35 postirradiation. The scoring systems for radiation-induced proctitis used the Vienna Rectoscopy Score (VRS) based on the endoscopic terminology of the World Organization for Digestive Endoscopy. It included a graduated description of endoscopic findings: telangiectasia, congested mucosa, ulceration, stricture, and necrosis [18]. One week after the last MSC injection, pigs were euthanized and anus, rectum, and colon (at least 3 cm distant from rectum) were removed for histologic and gene expression analysis.

### Isolation, Expansion, and Injection of Porcine MSCs

Bone marrow (30 ml) was collected from the humeral head of the pigs 12 days postirradiation. Autologous bone marrow mononuclear cells were seeded at 100,000 cells per  $\text{cm}^2$  in minimal essential medium- $\alpha$  ( $\alpha$ -MEM; Biological Industries) with 20% fetal bovine serum (A15-101; PAA Laboratories, Velizy-Villacoublay, France, <http://www.paa.at>) and 10 mg/ml ciprofloxacin (Ciflox, 400 mg/200 ml; BayerPharma, Puteaux, France, <http://www.bayerpharma.com>). After 72 hours, the adherent fibroblast-like cells (passage 0) were cultured until they reached 80%–90% confluence, with medium replacement every 3 days. Most of the nonadherent cells were washed off the flask during the first medium change. Adherent fibroblast-like cells were allowed to grow for 2 weeks in passage 0 (P0) and 1 week in passage 1 (P1). At the end of P0, 5%–10% of the cells expressed the CD45 marker, and at the end of P1, less than 5% expressed it. Adherent MSCs were harvested by trypsinization and grafter-suspended in saline solution (9% NaCl) prior to administration. Some cells were reseeded at a density of 4,000 cells per  $\text{cm}^2$  in passage 1. At confluence, half of the cells were injected (second administration) and the other half were cryopreserved (in  $\alpha$ -MEM, 9% albumin, 10% dimethyl sulfoxide) in order to perform a third injection 1 week later.

### Colony-Forming Unit Fibroblast Assays

To evaluate the potential of MSCs to form colonies, BM mononuclear cells were plated at 330,000 cells per 25-cm<sup>2</sup> flask at P0, and MSCs were plated at 200 cells per 25-cm<sup>2</sup> flask (P1). Cells were cultured for 10 days before ethanol fixation, Giemsa staining, and colony number recording.

### Flow Cytometry

Expression of MSC markers was studied by fluorescence-activated cell sorting. Cells were stained with CD90-PE (clone 5E10; BD Pharmingen, San Diego, CA, <http://www.bdbiosciences.com>), CD44-PE (clone MEM-263; Abcam, Cambridge, MA, <http://www.abcam.com>), CD29-fluorescein isothiocyanate (FITC) (clone MEM-101A; Abcam), swine leukocyte antigen SLA1-FITC (clone JM1E3; AbD Serotec, Raleigh, NC, <http://www.ab-direct.com>), CD105-PE (clone MEM-229; Abcam), and CD45-FITC (clone 1E4; AbD Serotec) antibodies. Isotype antibodies FITC- or PE-conjugated (clone W3/25; AbD Serotec) were included as controls. Cell staining was analyzed on a FACScalibur Cytometer (Becton, Dickinson and Company, Franklin Lakes, NJ, <http://www.bd.com>).

### Differentiation Assays

For osteogenic differentiation, porcine MSCs were grown for 14 days in  $\alpha$ -MEM supplemented with 100 nM dexamethasone (Sigma-Aldrich, St. Louis, MO, <http://www.sigmaaldrich.com>), 10 mM  $\beta$ -glycerophosphate (Sigma-Aldrich), 0.05 mM ascorbic acid (Sigma-Aldrich), 10 mg/ml ciprofloxacin, and 10% fetal bovine serum (PAA Laboratories). The presence of alkaline phosphatase activity was examined using a colorimetric assay (Vector Blue Alkaline Phosphatase Substrate Kit III; Vector Laboratories, Burlingame, CA, <http://www.vectorlabs.com>). Alizarin red S and von Kossa staining (Sigma-Aldrich) was used to identify the mineralized bone matrix deposition in cells. To evaluate adipogenic differentiation capacity, cells were grown in basal medium supplemented with 5 ng/ml epidermal growth factor (EGF), 0.5 ng/ml vascular endothelial growth factor (VEGF), 10 ng/ml FGF2, 20 ng/ml IGF1, 0.2  $\mu$ g/ml hydrocortisone, 1  $\mu$ g/ml ascorbic acid, 22.5  $\mu$ g/ml heparin, 1 $\times$  antibiotics (gentamicin and amphotericin B), and 2% fetal bovine serum (Lonza, Walkersville, MD, <http://www.lonza.com>). After 3 weeks, fixed cells were incubated with an Oil Red O solution (lipid droplet assay; Cayman Chemicals, Ann Arbor, MI, <http://www.caymanchem.com>) before examination. Chondrogenic differentiation was induced in cell masses in Dulbecco's modified Eagle's medium-high glucose (Gibco, Invitrogen, Saint Aubin, France, <http://www.invitrogen.com>) supplemented with 100 mM dexamethasone, 1 mM sodium pyruvate, 0.17 mM ascorbic acid, 0.35 mM L-proline, 1 $\times$  insulin-transferrin-selenium (Sigma-Aldrich), 5.33  $\mu$ g/ml linoleic acid (Sigma-Aldrich), 1.25 mg/ml human albumin (LFB Laboratories, Courtaboeuf, France), 10 mg/ml ciprofloxacin, and 10% fetal bovine serum (PAA Laboratories). After 21 days, cell masses were fixed, embedded, and sectioned with a microtome. Acidic mucopolysaccharides were stained with Alcian blue solution to demonstrate cartilage matrix production.

### Exposure to Hypoxia

A total of 5  $\times$  10<sup>6</sup> MSCs from each pig ( $n = 6$ ) were seeded in  $\alpha$ -MEM without serum in two 75-cm<sup>2</sup> flasks: one incubated at 37°C, 3% O<sub>2</sub>, and the other one incubated under normal conditions (37°C, 20% O<sub>2</sub>). Twenty-four hours poststimulation, supernatants and cellular lysates (lysis buffer: PBS containing 1%

Triton X-100 [Prolabo], 1% Tergitol-type Nonidet P40 [Sigma-Aldrich], 0.1% sodium dodecyl sulfate [Sigma-Aldrich], 0.5% sodium deoxycholate [Sigma-Aldrich], and 1% protease inhibitor cocktail [Sigma-Aldrich]) were collected for enzyme-linked immunosorbent assay (ELISA) analysis. The MSC supernatants were concentrated 10 times by ultrafiltration using 3-kDa molecular mass cutoff ultrafiltration membranes (Amicon Ultra-15; Millipore, Billerica, MA, <http://www.millipore.com>) following the manufacturer's instructions. The concentrations of cytokines, angiogenic factors, and matrix molecules in 10-fold concentrated culture supernatants and cellular extracts were determined using ELISA kits (MMP-9, keratocyte growth factor [KGF], and VEGF kits from Gentaur [Paris, France, <http://www.gentaur.com>] and interleukin [IL]-1, IL-6, MMP-2, TIMP-2, and endothelial nitric oxide synthase [eNOS] kits from Antibodies-Online.com [Atlanta, GA, <http://www.antibodies-online.com>]).

### Histological and Immunohistochemical Analysis

Dewaxed and rehydrated paraffin tissue sections (6  $\mu$ m) of anus, rectum, and colon were stained with hematoxylin-eosin-saffran. Collagen deposition was detected by Sirius red staining using standard methods. The heat-induced epitope retrieval pretreatment method was used for MMP-3 and MMP-14 antibodies, and pretreatment with trypsin was suitable for TIMP-1, TIMP-2, MMP-9, and S100A9 antibodies. For activated monocyte/macrophage detection, sections were successively incubated in proteinase K (20  $\mu$ g/ml in 10 mM Tris-HCl, pH 7.6) and with the monoclonal anti-MAC387 (Thermo Fisher Scientific, Illkirch, France, <http://www.thermofisher.com>). MMP-2 (NB2000-193; Acris, Montluçon, France, <http://www.acris-antibodies.com>), MMP-3 (AP00226-PU-N; Acris), MMP-9 (NB-100-78557; Acris), MMP-14 (Ab6004; Millipore), TIMP-1 (AF2310; Acris), TIMP-2 (Mab13446; Millipore), and S100A9 (Ab62227; Abcam) were immunolocalized. MMP-3 immunolocalization was performed using the streptABC-HRP system (DakoCytomation, Trappe, France, <http://www.dakocytomation.com>), and the EnVision<sup>+</sup> System horseradish peroxidase (HRP) (DakoCytomation) was used as secondary reagent for all immunostaining sections. The color reaction was developed using the NovaRED kit (Vector Laboratories, Burlingame, CA, <http://www.vectorlabs.com>) and counterstained with Mayer's hemalun. The vascular and cellular densities were measured using image analysis software (HistoLab; Microvision Instruments, Evry, France, <http://www.microvision.fr>).

### Real-Time Polymerase Chain Reaction Analysis

Total RNA was extracted from the anus, rectum, and colon with the RNeasy Mini kit (Qiagen, Hilden, Germany, <http://www.qiagen.com>), and cDNA was prepared with the SuperScript RT Reagent Kit (Applied Biosystems, Foster City, CA, <http://www.appliedbiosystems.com>). Real-time polymerase chain reaction (PCR) was performed on an ABI Prism 7000 Sequence Detection System. PCR was carried out with SYBR Green PCR Master Mix (Applied Biosystems). The primer sequences are listed in supplemental online Table 2. For TLR2, 4, 5, 9, CD163, and FGF2, TaqMan primers and probes were from Applied Biosystems. Glyceraldehyde-3-phosphate dehydrogenase (GAPDH) was quantified as an internal control. Transcript levels of target genes were calculated using the 2<sup>- $\Delta\Delta$ Ct</sup> method, and irradiated MSC-treated animals were compared with irradiated animals.

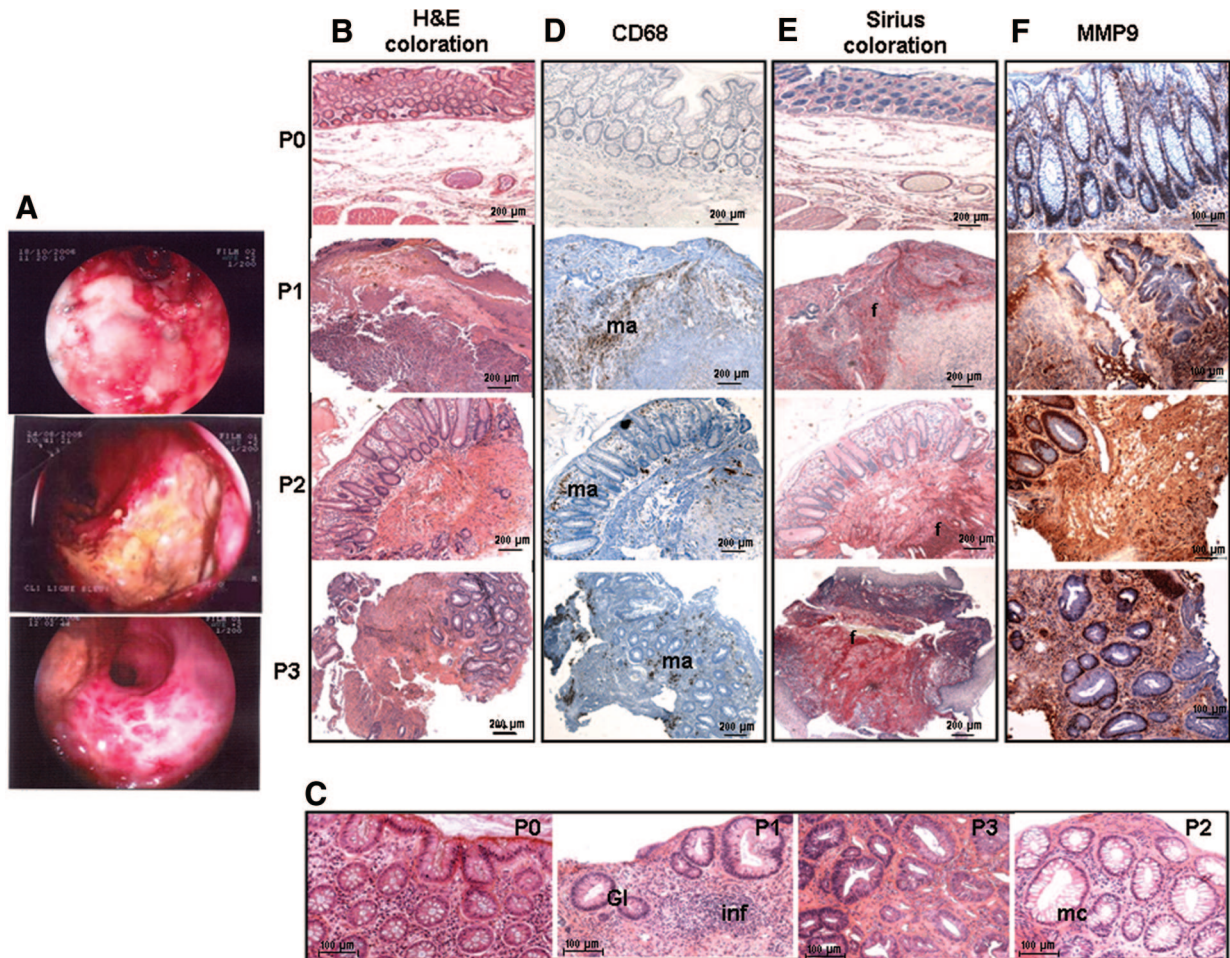


**Figure 1.** Rectal damage in tissues from patients treated for prostate cancer. **(A):** Endoscopy of three overexposed patients. **(B):** Rectal morphology: H&E-stained paraffin sections. **(C):** Gland loss, inflammatory cell infiltration, and mucus-secreting cells (magnification,  $\times 10$ ). **(D):** CD68 immunostaining showing macrophage infiltration. **(E):** Sirius red staining showing fibrosis. **(F):** MMP-9 immunostaining. Abbreviations: f, fibrosis; Gl, gland loss; H&E, hematoxylin and eosin; inf, inflammatory cell infiltration; ma, macrophage infiltration; mc, mucus-secreting cells; MMP9, matrix metalloproteinase; P, patient.

### ELISA Tests

C-reactive protein (CRP) concentration in blood samples was determined by specific ELISA (Eurobio-Abcys, Courtaboeuf, France, <http://www.eurobio.fr>).

### Statistics

Data are expressed as mean  $\pm$  SEM. One-way analysis of variance was used followed by a Bonferroni post test to determine the significance of differences. *p* values less than .05 were considered statistically significant.

## RESULTS

### Overexposed Patients Develop Severe Proctitis

We undertook a retrospective histological study in three patients treated with radiotherapy for prostate cancer where 25% of the rectum received more than 70 Gy. Between 1 and 2 years after exposure, colonoscopy showed congested mucosa, telangiectasia, and large area of fibrosis (Fig. 1A). As compared with nonirradiated rectum (patient 0), microscopic images revealed depletion of crypts with shortening and narrowing (Fig. 1B). A prominent loss of crypts was observed in overexposed rectum as

compared with control (Fig. 1C). Mucus-secreting cells were absent in patients 1 and 3 but abundant in patient 2. The submucosae showed edema associated with muscularis mucosae disorganization and a large leukocyte infiltration in the lamina propria. Immunostaining of the CD68 antigen showed a high macrophage density as compared with nonirradiated rectum, mainly localized beneath the epithelium in close proximity to and intermingled with other inflammatory cells in the lamina propria (Fig. 1D). Sirius staining revealed large fibrotic areas in the muscularis layer (Fig. 1E). MMP-9 immunostaining increased in the epithelial cells and submucosal inflammatory cells as compared with control (Fig. 1F).

### Porcine MSC Production and Characterization

The pig-derived MSCs presented a characteristic spindle shape (Fig. 2A) and reached confluence by day 14 at passage 0 and day 7 at passage 1 (Fig. 2B). Colony-forming units-fibroblast assays indicated that the percentages of colonies were approximately 0.0043% in passage 0, 17.18% in passage 1, and 13.17% in passage 2 (Fig. 2C). Flow cytometry analysis at passage 1 revealed that cells were positive ( $>90\%$ ) for CD90, CD29, CD44, and SLA-1 surface markers and negative ( $<2\%$ ) for CD45. CD105 was expressed in about three-quarters of them (Fig. 2D). As shown in Figure 2E, when cultured in

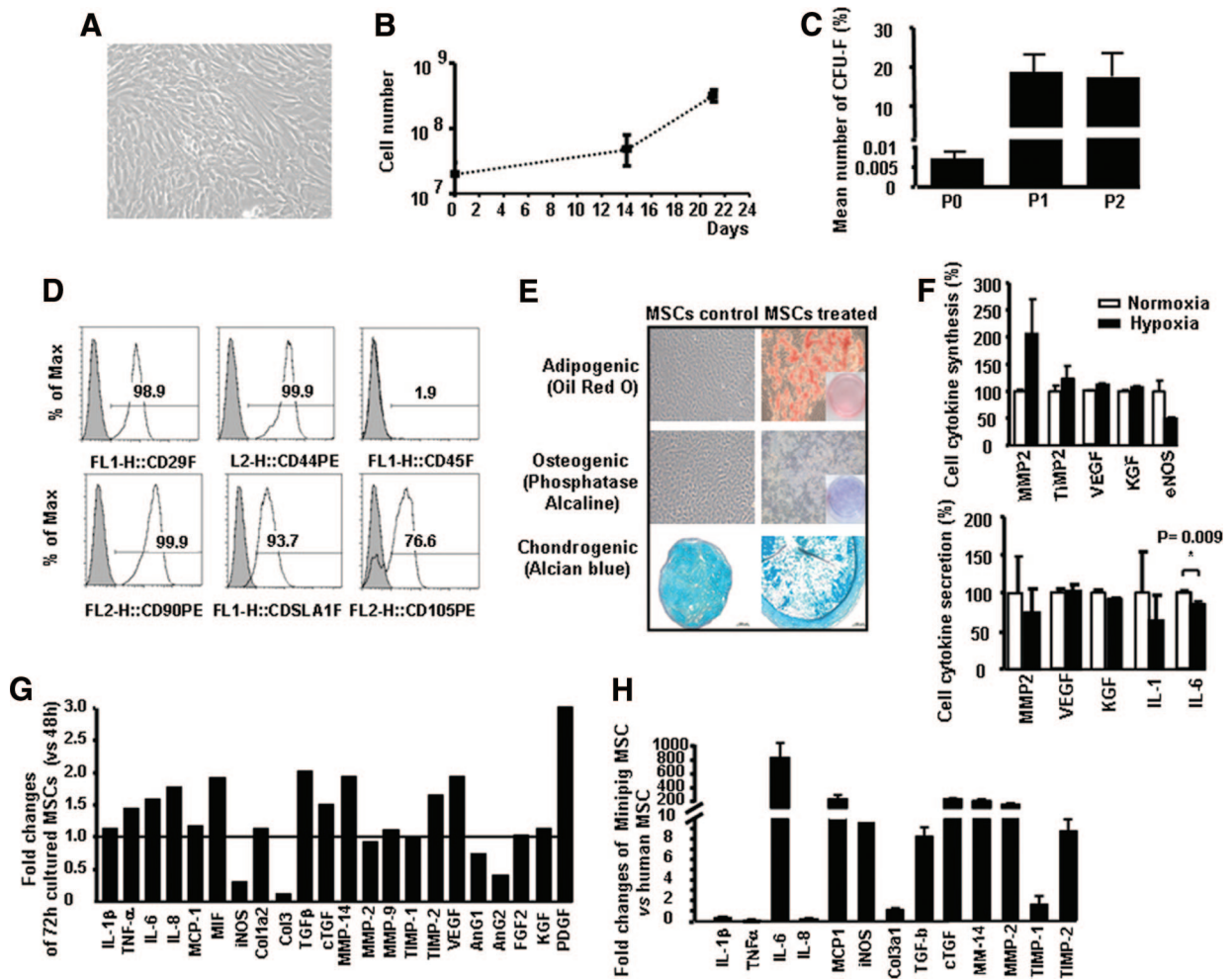


**Figure 2.** Porcine MSC characterization. (A): Morphology at P1. (B): Proliferative capacity. (C): Clonogenicity. (D): Phenotype. (E): Differentiation. (F): Protein synthesis and secretion capacity of porcine MSCs (pMSCs) in normoxia and hypoxia. (G, H): Cultured pMSC factor expression. The fold changes were generated by comparing pig MSCs with human MSCs cultured in the same conditions. Glyceraldehyde-3-phosphate dehydrogenase was quantified as an internal control. Abbreviations: CFU-F, colony-forming units-fibroblast; cTGF, connective tissue growth factor; eNOS, endothelial nitric oxide synthase; IL, interleukin; iNOS, inducible nitric oxide synthase; KGF, keratocyte growth factor; MIF, macrophage migration inhibitory factor; MMP, matrix metalloproteinase; MSC, mesenchymal stem cell; P, passage; TGFβ, transforming growth factor-β; TNF, tumor necrosis factor; VEGF, vascular endothelial growth factor.

osteogenic, adipogenic, and chondrogenic media, cells differentiated into osteoblasts, adipocytes, and chondrocytes. To understand the potential paracrine effect of MSCs, their synthesis and secretion of inflammatory, remodeling, and angiogenic factors after hypoxia stimulation (3% oxygen) and serum deprivation for 24 hours were investigated (Fig. 2F). Culture of MSCs under hypoxia had a tendency to induce VEGF protein expression ( $p = .05$ ), although the expressions of MMP-2, TIMP-2, KGF, and eNOS were unchanged. Furthermore, hypoxia inhibited IL-6 secretion ( $p < .01$ ) without changing IL-1, MMP-2, VEGF, and KGF secretions. MMP-9, IL-1β, and IL-6 synthesis and MMP-9, TIMP-2, and eNOS release from normoxia- or hypoxia-stimulated mesenchymal cells was undetectable. Expression levels after 72 hours of cultured BM-MSCs revealed an increase of inflammatory factors (IL-6, IL-8, macrophage migration inhibitory factor [MIF]), remodeling factors (transforming growth factor-β [TGF-β], MT1-MMP, TIMP-2), and angiogenesis (VEGF, platelet-derived growth factor [PDGF]) compared with 48 hours of cultured BM-MSCs (Fig. 2G). Compared with human MSCs cultured in the same conditions, real-time PCR analysis showed that minipig MSCs expressed considerably greater amounts of IL-6, monocyte chemoat-

tractant protein-1 (MCP-1), and remodeling factors (TGF-β, MMP-2, MMP-14, TIMP-1, TIMP-2) (Fig. 2H).

### Repeated MSC Injections Control Systemic and Local Inflammation

In our pig model, the MSC treatment reduced the elevation of white blood cell number (Fig. 3A) and the C reactive protein (CRP) concentration in serum (Fig. 3B) induced by irradiation. The stool score increased in most pigs, beginning at day 7 postirradiation. Bleeding appeared between day 4 and day 7 (Fig. 3C). MSC injections considerably ameliorated the stool score. Endoscopy showed a large fibrotic area and friability in the rectum at day 15 postirradiation (Fig. 3D). According to VRS [18], the minipig endoscopies showing stricture grade  $\geq 2$ , and the presence of necrosis suggested a grade 5 of the endoscopic severity. The MSC treatment considerably reduced the extent of fibrosis 1 week after two MSC injections. The mucosa appeared supple without telangiectasia and erythema, comparable to a nonirradiated pig. Macroscopic observation confirmed extensive fibrosis in the rectum and submucosal edema in irradiated pigs (Fig. 3E), and the cross-sectional view showed a marked thickening

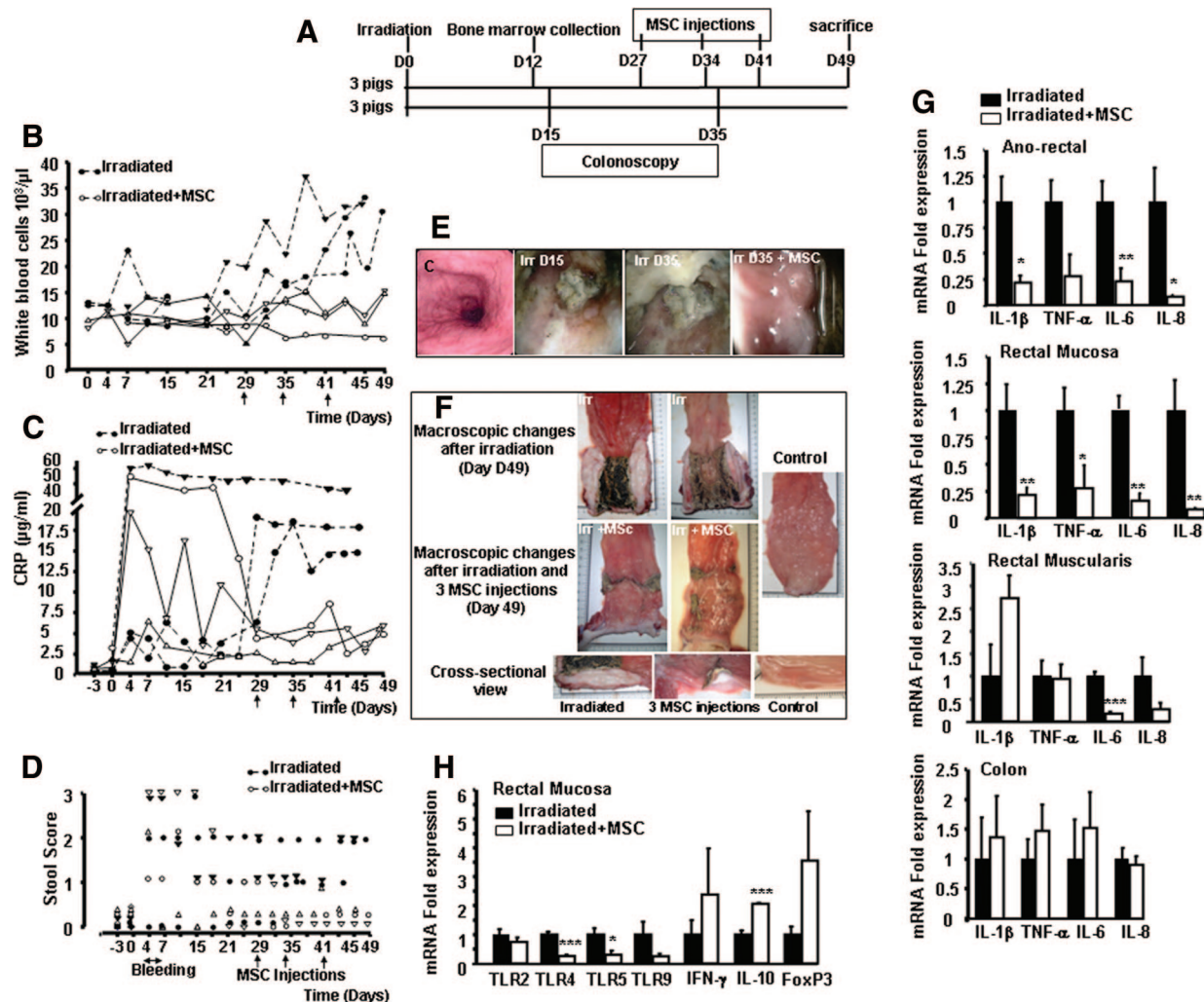


**Figure 3.** Experimental efficacy and anti-inflammatory effect of MSC injections. **(A):** Experimental design. **(B):** White blood cell counts. **(C):** Serum CRP concentration. **(D):** Stool score during protocol in three irradiated pigs (closed symbols) and three irradiated MSC-treated pigs (open symbols). **(E):** Endoscopy at days 15 and 35 postirradiation. **(F):** Representative macroscopic pictures of rectum and colon at day 49 after irradiation and irradiation-MSC injections. **(G, H):** Real-time polymerase chain reaction analysis of inflammatory mediators **(G)** and factors related to immunity **(H)**. The fold changes were generated by comparing irradiated-MSC-treated animals with irradiated animals. *p* values with Bonferroni correction were as follows: \*, *p* < .05; \*\*, *p* < .01; \*\*\*, *p* < .001 for irradiated-MSC-treated pigs versus irradiated pigs. Abbreviations: C, control; CRP, C-reactive protein; D, days; IL, interleukin; Irr, irradiated; MSC, mesenchymal stem cell; TLR, Toll-like receptor; TNF- $\alpha$ , tumor necrosis factor- $\alpha$ .

of the muscle layer. Three MSC injections reduced fibrosis, and muscle layer thickening was much less marked in the rectum.

We used real-time PCR to evaluate the local anti-inflammatory effect of systemic MSC treatment (Fig. 3F). As compared with the irradiated pigs, expressions of tumor necrosis factor- $\alpha$  (TNF- $\alpha$ ), IL-6, and IL-8 were significantly downregulated in the anorectum and the rectal mucosae. Given the influence of MSCs on innate immunity, Toll-like receptor (TLR) expression was examined after three MSC injections. As compared with irradiated pigs, expression of TLR-4 and TLR-5 was significantly reduced in the rectal mucosae. In addition, three MSC injections induced a twofold increase of the anti-inflammatory cytokine IL-10 expression and promoted infiltration of regulatory T cells (Tregs), demonstrated as specific transcriptional factor FoxP3 expression elevation (Fig. 3G).

Another feature of MSCs' effect on immunity relates to the interaction with macrophages. As shown in Figure 4A, representative MAC387 immunostaining showed increased macrophage density in the rectum and colon of irradiated pigs as compared

with that of nonirradiated pigs. The stained macrophages were mainly localized beneath the epithelium and in close proximity to the vessels (Fig. 4B). After three MSC injections, the number of MAC387-positive macrophages decreased greatly in the rectal and colonic mucosae in MSC-treated pigs as compared with irradiated pigs (Fig. 4C), confirmed by S100A9 immunostaining. In addition, real-time PCR analysis showed MCP-1 repression in the anorectum, rectum, and colon after three MSC injections (Fig. 4D). Inducible nitric oxide synthase (iNOS) expression reflecting macrophage activity was repressed in all tissues after three MSC injections. Interestingly, the M2 macrophage phenotype based on CD163 expression was overexpressed in the rectal mucosae of MSC-treated pigs.

**Repeated MSC Injections Modulate Extracellular Matrix**

To assess the effect of MSCs on rectal fibrosis induced by irradiation, we examined collagen deposits with the Sirius red collagen assay. As shown in Figure 5A, representative morphological analysis of collagen (Col) accumulation revealed a net collagen deposition in the

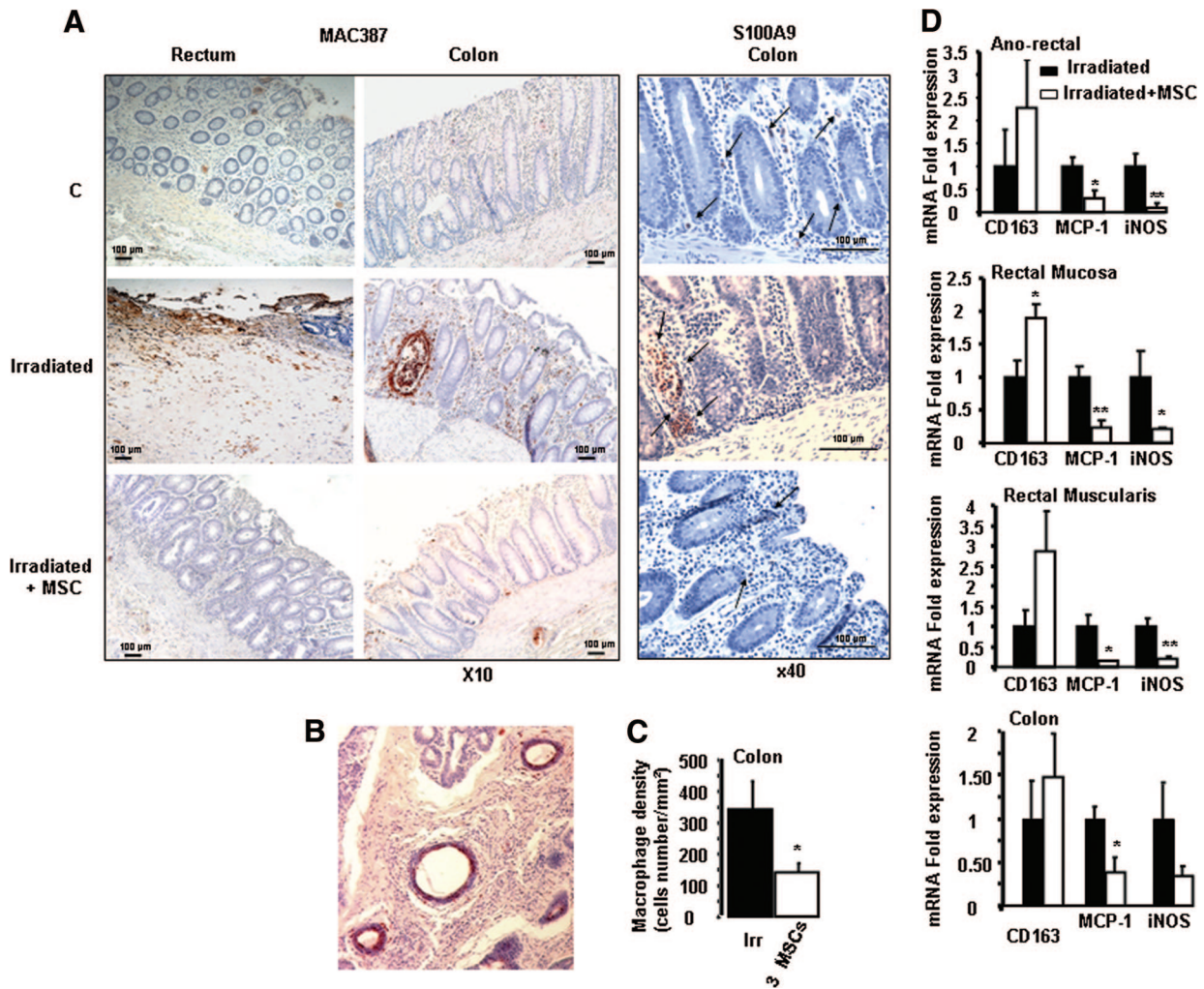


**Figure 4.** MSC effect on macrophage infiltration. (A): Immunostaining for MAC387-positive macrophages and S100A9. (B): Macrophage immunostaining localized beneath the epithelium and in close to blood vessels. (C): Colonic MAC387-positive cell quantification. (D): Real-time polymerase chain reaction analysis of genes related to macrophage activity. *p* values calculated by analysis of variance with Bonferroni correction were as follows: \*, *p* < .05; \*\*, *p* < .01 for irradiated-MSC-treated pigs versus irradiated pigs. Abbreviations: C, control; iNOS, inducible nitric oxide synthase; Irr, irradiated; MCP-1, monocyte chemoattractant protein-1; MSC, mesenchymal stem cell.

rectum of irradiated pigs. After three MSC injections the collagen deposits were decreased, reducing the extent of fibrosis. Real-time PCR analysis confirmed the significant reduction of col1a2 and col3a1 expression in the anus and rectal mucosae in three MSC-treated pigs (Fig. 5B). In accordance with this result, expression of the fibrotic mediators TGF-β and connective tissue growth factor was repressed (fourfold) in the rectal mucosae of three MSC-treated pigs as compared with irradiated pigs. In addition, analysis of the KGF expression involved in the restoration of mucosal integrity showed a marked increase of the mRNA level in the rectal mucosae and the colon (3- and 9.5-fold, respectively) as compared with irradiated pigs.

The balance between MMPs and their endogenous inhibitors (TIMPs) is of significance in determining the extent of fibrosis. In the rectum, immunostaining of MMPs and TIMPs showed a net reduction of MMP-3, MMP-9, MMP-14, TIMP-1, and TIMP-2 immunodetection without modification of MMP-2 immunostaining after MSC injections (Fig. 6). Real-time PCR analysis confirmed the drastic repression of MMP-3, MMP-9, MMP-14, and TIMP-2 in MSC-treated pigs, whereas TIMP-1 was not modified. Because the balance of collagen synthesis, collagen degradation by MMPs, and inhibition of

MMPs by TIMPs regulates collagen deposition, the net collagen deposition was assessed in MSC-treated pigs using the collagen-to-MMP-to-TIMP ratio adapted to radiation enteritis [19]. Based on real-time PCR results, the collagen mRNA value was divided by the fold change value for the relevant MMPs and TIMPs. The resulting fold changes in MSC-treated pigs were generated by comparison with irradiated nontreated pigs (Fig. 6C). Hence, values lower than 1 reflect collagen degradation relative to the fibrotic state. Results showed a net reduction of collagen deposition after three MSC injections. In the colon (supplemental online Fig. 1), immunostaining and real-time PCR analysis showed that MSC injections reduced expression of MMP-9 without a change in TIMP-1 and TIMP-2 expression. The net collagen/MMP:TIMP ratio was markedly reduced in MSC-treated pigs.

### Repeated MSC Injections Regulate Factors Implicated in Angiogenesis

Real-time PCR analysis of eNOS, VEGF, FGF2, and PDGF reflecting angiogenesis did not show any change in the expression of these markers in the anus of MSC-treated pigs as compared with

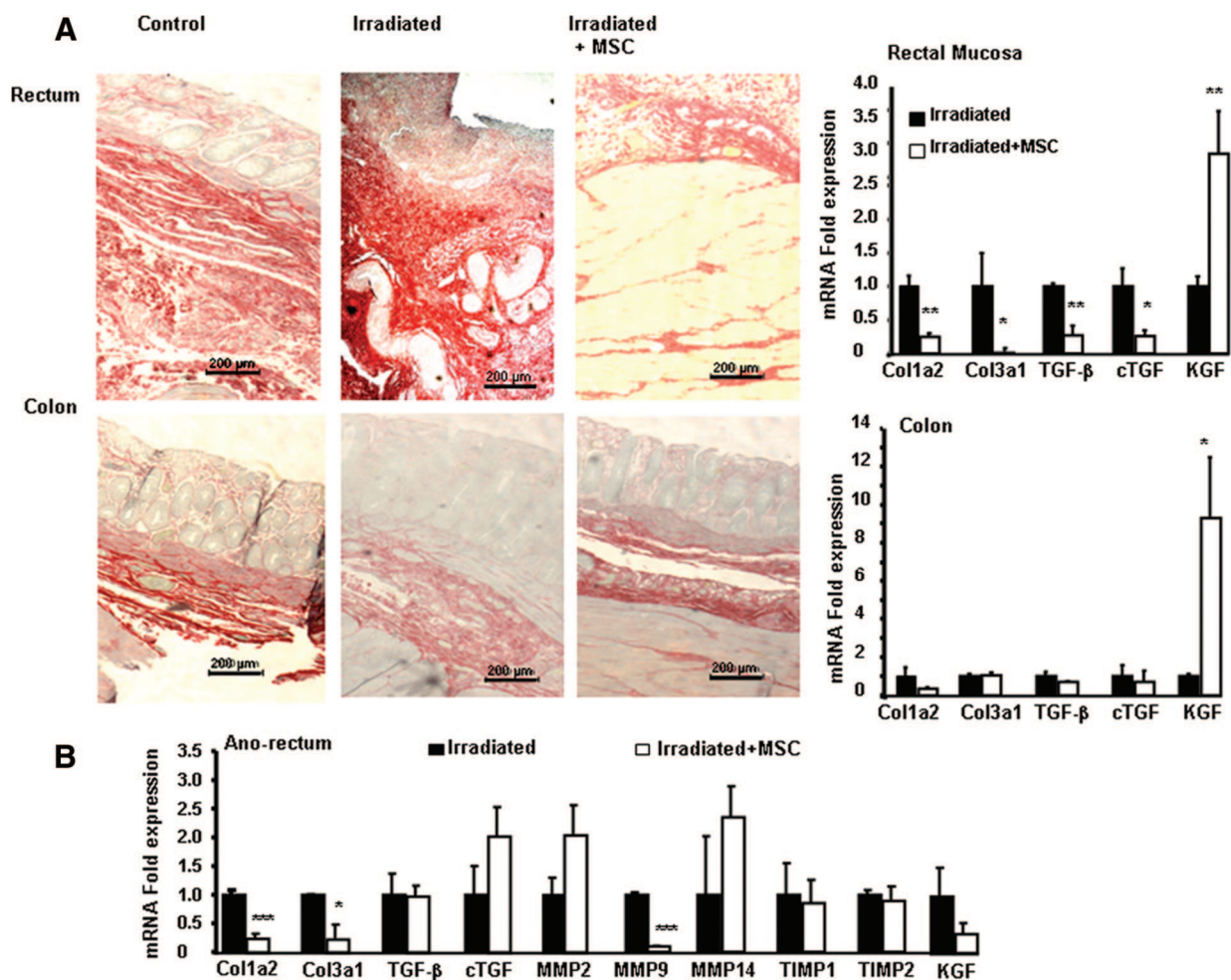


**Figure 5.** MSC injections reduced fibrosis. **(A):** Photomicrographs of rectum and colon sections stained with Sirius red (magnification,  $\times 10$ ). **(B):** Real-time polymerase chain reaction analysis of genes related to fibrosis. The fold changes were generated by comparing irradiated MSC-treated animals with irradiated animals. *p* values calculated by analysis of variance with Bonferroni correction were as follows: \*, *p* < .05; \*\*, *p* < .01; \*\*\*, *p* < .001 for irradiated-MSC-treated pigs versus irradiated pigs. Abbreviations: cTGF, connective tissue growth factor; KGF, keratocyte growth factor; MMP, matrix metalloproteinase; MSC, mesenchymal stem cell; TGF- $\beta$ , transforming growth factor- $\beta$ ; TIMP, tissue inhibitor of metalloproteinase.

irradiated pigs (Fig. 7A). In the rectal mucosa, MSC injections induced 3.5- and 3-fold increases in VEGF and VEGF receptor 2 (VEGFR2) expression, respectively, when angiopoietin (Ang1, Ang2), FGF2, and PDGF were repressed as compared with irradiated pigs. In the colon, marked increases of eNOS, VEGF, VEGFR1, and PDGF were observed. The ratio analysis of vascular area to rectal submucosae area showed that MSC injections led to a 1.6-fold decrease of the vascular density when a 2-fold increase was observed in the rectal muscularis (Fig. 7B, 7C).

## DISCUSSION

The effective management of proctitis in patients undergoing very-high-dose conformal radiotherapy has become a major focus for clinicians, notably with a dose escalation where 25%–30% of the rectal volume receives more than 70 Gy. In this study, histologic analyses of these patients showed that overexposure induced an accumulation of inflammatory cells in the irradiated area and that progression of fibrosis may result in stricture or fistula formation, as previously described [3]. The advent of regenerative medicine based on cellular therapy has focused on the attractive properties of

MSCs in promoting regeneration of injured tissues. Bone marrow-derived MSCs contribute to tissue repair by differentiation into vascular smooth muscle cells, endothelial cells, pericytes, or epithelial cells [14–16, 20]. In this report, we demonstrate in a preclinical model the potential efficacy of MSC injections in anorectal fibrosis induced by high doses of radiation. We show that repeated systemic injections of autologous MSCs modulated the anorectal inflammatory response and stimulated extracellular matrix (ECM) remodeling, thereby helping to reduce fibrosis.

For this study, porcine MSCs derived from bone marrow expressed mesenchymal cell surface markers and were capable of multiple mesodermal differentiations (adipocytes, osteoblasts, and chondrocytes). The culture conditions and the phenotype of the porcine MSCs were similar to those of human MSCs isolated to treat patients suffering radiation skin burns, where CD45-positive cells are rapidly eliminated from the culture [21]. Moreover, cultured porcine MSCs in hypoxic conditions as compared with normal conditions (normoxia) produced VEGF protein, which is involved in neovascularization, and inhibited IL-6 release.

In our model, pigs received a high single dose of radiation (between 21 and 29 Gy) delivered to the rectum. Previous animal

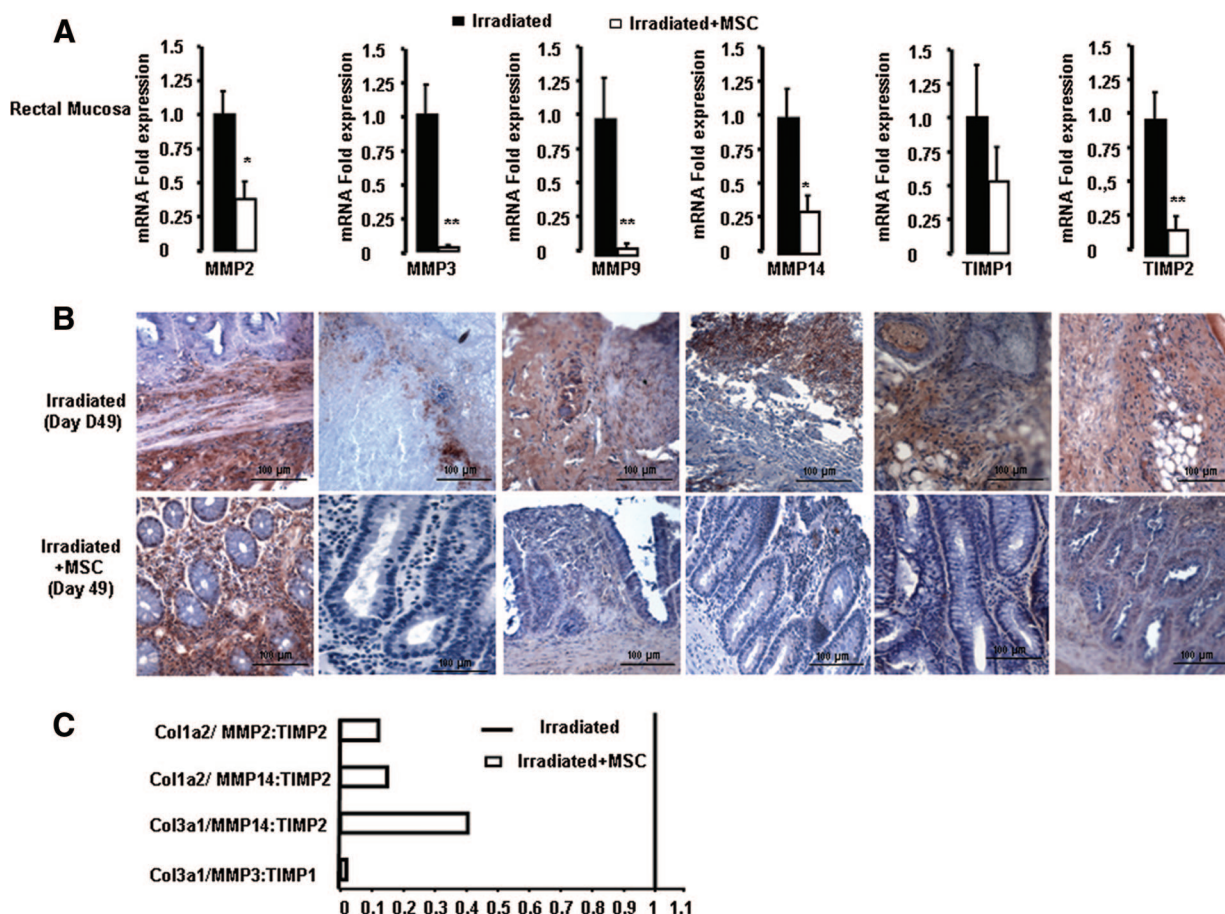


**Figure 6.** Rectal extracellular matrix remodeling. **(A):** Real-time polymerase chain reaction of MMPs and TIMPs. **(B):** MMP and TIMP immunostaining. **(C):** Collagen-to-MMP-to-TIMP ratio. Relative expression of MMP was calculated by determining the fold change of MMP mRNA levels relative to its relevant inhibitor TIMP in MSC-treated pigs (histograms) compared with irradiated pigs (baseline). \*,  $p < .05$ ; \*\*,  $p < .01$  for irradiated-MSC-treated pigs versus irradiated pigs. Abbreviations: MMP, matrix metalloproteinase; MSC, mesenchymal stem cell; TIMP, tissue inhibitor of metalloproteinase.

model studies showed that a rapid increase in the severity of the pathological changes was observed between 20 and 30 Gy delivered in a single dose (ulceration, fibrosis, and vascular sclerosis), which, in many ways, parallels the histological changes to the late rectal toxicity described in human receiving overdosage [22]. There is an increasing body of evidence linking acute and late effects in the rectum following radiotherapy for prostate cancer. The association between acute and late effects is important, particularly if the potential exists to modify acute and therefore late toxicity [22]. This model of localized single-dose radiation exposure generates histopathological lesions similar to those seen clinically during the severe chronic phase (i.e., severe acute mucosal ulceration and transmural collagen deposition). In our preclinical model, the MSC treatment was performed on established lesions specific to chronic proctitis and characterized by fibrogenesis. Therefore, our therapeutic intervention is viewed as prevention for chronic proctitis. For this study the number of cells injected ( $2 \times 10^6$  MSCs per kilogram) intravenously was based on intravenous MSC treatment in some clinical studies [9]. Some studies have reported that intravenously injected MSCs are initially trapped in the lungs [23], but other studies suggest that pulmonary trapping of MSCs following intravenous administration is only a transient phenomenon. The kinetics of trapped MSCs in lung showed 50%–60% pulmonary

accumulation of MSCs 1 hour after the injection with a subsequent decrease to approximately 30% 3 hours postinjection [24]. Finally, MSCs are found in the irradiated tissue [25].

We showed for the first time that MSC injections considerably reduced the severity of inflammation-related anorectal and colonic injuries induced by overexposure, by both reducing macrophage infiltration and downregulating expression of inflammatory cytokines, as reflected by normalization of plasma CRP level. Interestingly, we observed overexpression of CD163 in the rectum. CD163 is highly indicative of M2 type macrophages involved in the downregulation phase of acute/chronic inflammation and resulted in constructive remodeling of the abdominal wall: organized collagenous connective tissue, wound healing, and angiogenesis. In parallel, iNOS expression, reflecting the strength of activated M1 type macrophages, the proinflammatory population perpetuating the inflammatory response [26], was repressed in all tissue after MSC injections. These results add weight to the anti-inflammatory properties of MSC injections, with a shift of macrophage phenotype, which could help set the stage for tissue repair. Macrophages may be programmed by their microenvironment to mediate locally destructive effects or to produce a range of anti-inflammatory, proregenerative factors [27]. Recent studies have shown that MSCs are involved in the reprogramming of macrophages, notably by enhancing IL-10 production [28]. In our study MSC injections reduced the

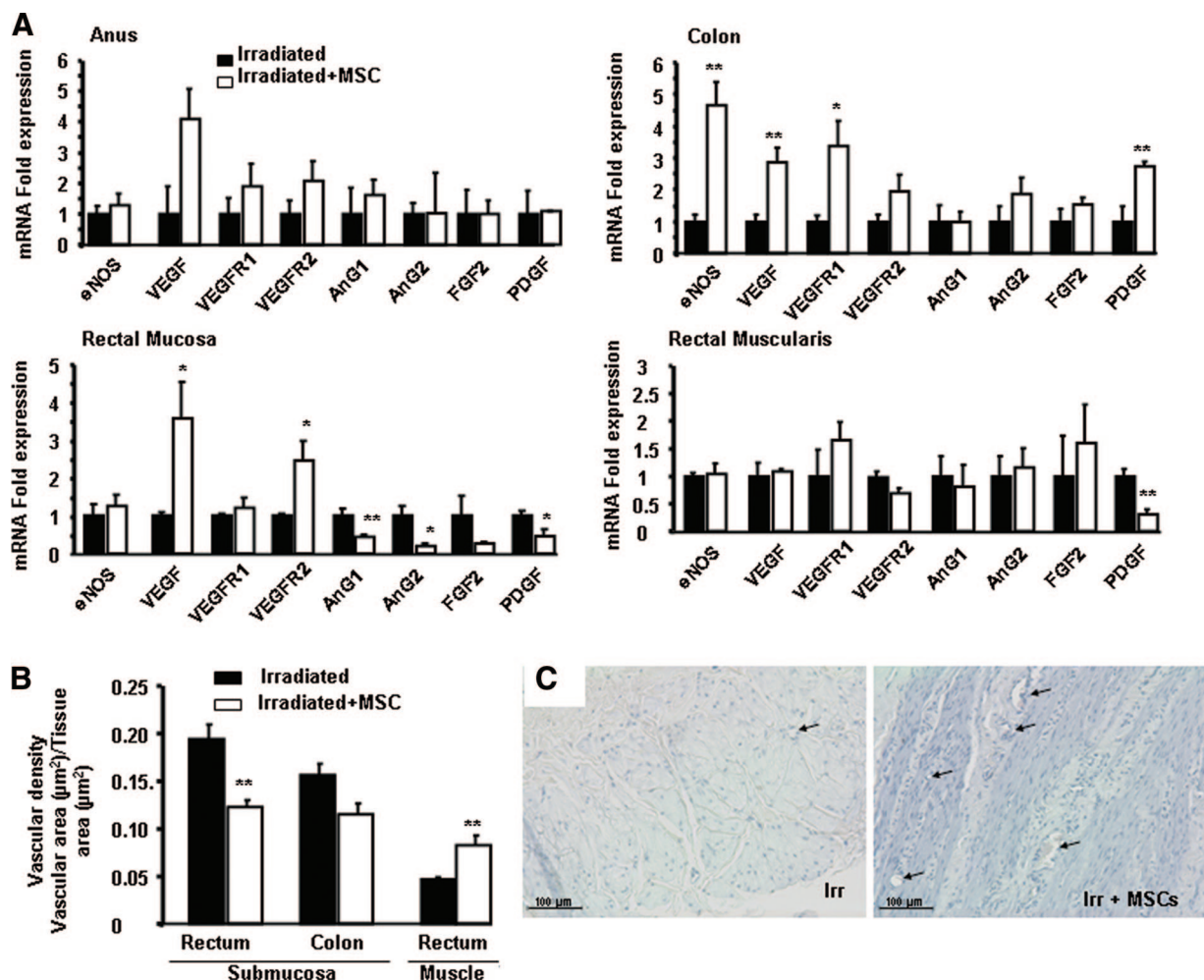


**Figure 7.** Angiogenesis effect of MSCs. **(A):** Real-time polymerase chain reaction analysis of angiogenic factors. **(B):** Computerized morphometric analysis of the vasculature sections was done for the total number of vessels per field (vascular area  $[\mu\text{m}^2]/\text{area} [\mu\text{m}^2]$ ). *p* values calculated by analysis of variance with Bonferroni correction were as follows: \*, *p* < .05; \*\*, *p* < .01 for irradiated-MSC-treated pigs versus irradiated pigs. **(C):** Vascular density photomicrographs in rectal muscles (arrows: vessels). Abbreviations: Ang, angiopoietin; eNOS, endothelial nitric oxide synthase; FGF, fibroblast growth factor; Irr, irradiated; MSC, mesenchymal stem cell; PDGF, platelet-derived growth factor; VEGF, vascular endothelial growth factor.

severity of radiation-induced inflammation, probably by reducing infiltrates of macrophages and changing their phenotype, and by promoting the generation/activation of Tregs characterized by Foxp3, following IL-10 expression. MSC-mediated immunomodulation occurs by multiple redundant pathways, of which Treg induction is only one [27]. Interestingly, we observed that MSC injections repressed the majority of TLRs in the rectal mucosa. Aberrant or dysfunctional TLR signaling may impair commensal-mucosal homeostasis, thus contributing to amplification and perpetuation of tissue injury. In particular, TLR4 is significantly increased in active disease states of both human Crohn’s disease and ulcerative colitis, an aberrant state of TLR activation [29]. Since activation of TLRs critically initiates the inflammatory and subsequent adaptive immune response [30], the TLR downregulation by MSC injections can limit or abrogate chronic inflammation.

A second key mechanism observed was that MSC injections resulted in reduction or limitation of anorectal fibrosis. Intense ECM remodeling seems to particularly affect intestinal mucosae in radiation enteritis, as previously shown [19]. Increased expression of MMP-2, MMP-3, and MMP-14 in mucosa may be involved in epi-

thelium activation and mediate activation of the fibrogenic signal. The concomitant induction of TIMPs counterbalances the induction of MMPs, leading to a net collagen deposition. In this study, immunostaining associated with real-time PCR analysis showed for the first time that MSC injections reduce expression of MMP-2, MMP-3, MMP-9, MMP-14, and TIMP-1. A close correlation has been demonstrated between elevated MMP mRNA with col3 expression and the extent of inflammatory cell infiltration in radiation enteritis [19]. Recent studies have demonstrated that macrophage depletion at the onset of fibrosis resolution could retard ECM degradation [31], suggesting that one phenotype of macrophages is essential for initiating ECM degradation, by producing MMPs. In addition, a causal relationship between TIMP elevation and fibrosis has been established in lung fibrosis induced by bleomycin, where TIMP-1 and TIMP-2 were elevated, and reduced after MSC treatment [32]. The net deposition of collagen occurs when the balance between TIMPs and MMPs tips in favor of TIMPs, whereas resolution is associated with reduced TIMP expression. In radiation enteritis the collagen to MMP to TIMP ratio is elevated [19]; conversely, in our preclinical

model this ratio was greatly reduced after three MSC injections as compared with irradiated pigs, demonstrating a reduction of fibrosis.

There is important interplay between angiogenesis, vascular remodeling, and fibrosis [33, 34]. Wu et al. [35] suggested that MSC treatment enhances wound healing through angiogenesis. In our preclinical study, an increase of VEGF expression was observed when AnG1 and AnG2 were repressed, associated with vascular density reduction in rectal mucosae. The role of angiogenesis and of proangiogenic factors in the pathophysiology of fibrosis is currently not understood. Angiogenesis might contribute to fibrosis [34, 36]. Abdollahi et al. [37] showed that inhibition of PDGF signaling attenuates the onset and development of radiation-induced lung fibrosis and has a significant survival benefit in mouse, which supports the concept of the concerted action of several factors in fibrosis. In particular, FGF2 is an important factor in myofibroblast migration, and blockade of both pathways might be required for an antifibrotic effect [38]. Likewise, the high antifibrotic efficacy of MSC injections might be explained in part by a net FGF2 and PDGF repression in the mucosae. The importance of PDGF signaling in the fibrotic process is provided by reports showing that some fibrogenic mediators, such as TGF- $\beta$ , IL-1, TNF- $\alpha$ , and FGF2, exhibit PDGF-dependent profibrotic activities [38]. The net reduction of inflammatory mediators by MSC injections also clearly helps to reduce fibrosis in other models [34].

In addition, evidence is needed showing that the injected stem cells are not conducive to teratoma formation, oncogenic transformation, or even the resumption of tumor growth after complete tumor sterilization. Some meta-analysis of clinical trials has reported the use of cultured MSCs without any reported confounding side effects related to the cell therapy [39]. Furthermore, the follow-up of patients after cell therapy treatments after radiotherapy for breast [40], bladder, or prostate cancer [41] has never revealed side effects.

## CONCLUSION

Fibronecrosis, fistulae, hemorrhage, and occlusion-referred late radiation response in humans have an important clinical impact in terms of persistence, morbidity, and mortality. Our preclinical model reinforces that systemic MSC therapy represents a promising strategy for patients suffering from severe and refractory irradiation-induced proctitis and/or radionecrosis. MSC therapy involves three mechanisms— inflammatory modulation, ECM remodeling, and proangiogenic effect—and probably promotes fibrosis regression when MSCs are injected repeatedly. Allogeneic MSC therapy can be proposed for patients experiencing proctitis of grade II or greater and refractory to nonsurgical interventions (anti-inflammatory agents, formalin, laser cauterization, or hyperbaric oxygen therapy). In fact, this innovative treatment based on MSC injection is currently proposed as compassionate therapy in patients suffering from refractory chronic irradiation-induced hemorrhagic colitis and fistula [41]. This study points the way to a potential new approach for the effective management of irradiation-induced severe proctitis.

## AUTHOR CONTRIBUTIONS

C.L.: conception and design, data collection, data analysis and interpretation, manuscript writing, final approval of manuscript; E.B. and M.P.: cell technical issue; V.H., C.S., J.-V.L.-L., B.L., and P.D.: technical support; J.-C.S., J.-M.S.: provision of patient material and critical revision for human-related content; M.B.: animal assistance; J.-J.L. and M.B.: study concept, manuscript revision, final approval of manuscript.

## DISCLOSURE OF POTENTIAL CONFLICTS OF INTEREST

The authors indicate no potential conflicts of interest.

## REFERENCES

- Zelesky MJ, Levin EJ, Hunt M et al. Incidence of late rectal and urinary toxicities after three-dimensional conformal radiotherapy and intensity-modulated radiotherapy for localized prostate cancer. *Int J Radiat Oncol Biol Phys* 2008;70:1124–1129.
- Eifel PJ, Levenback C, Wharton JT et al. Time course and incidence of late complications in patients treated with radiation therapy for FIGO stage IB carcinoma of the uterine cervix. *Int J Radiat Oncol Biol Phys* 1995;32:1289–1300.
- Garg AK, Mai WY, McGary JE et al. Radiation proctopathy in the treatment of prostate cancer. *Int J Radiat Oncol Biol Phys* 2006;66:1294–1305.
- Gilinsky NH, Burns DG, Barbezat GO et al. The natural history of radiation-induced proctosigmoiditis: An analysis of 88 patients. *Q J Med* 1983;52:40–53.
- Yegappan M, Ho YH, Nyam D et al. The surgical management of colorectal complications from irradiation for carcinoma of the cervix. *Ann Acad Med Singapore* 1998;27:627–630.
- Ash D. Lessons from Epinal. *Clin Oncol (R Coll Radiol)* 2007;19:614–615.
- Phinney DG, Prockop DJ. Concise review: Mesenchymal stem/multipotent stromal cells: The state of transdifferentiation and modes of tissue repair: Current views. *STEM CELLS* 2007;25:2896–2902.
- Chanda D, Kumar S, Ponnazhagan S. Therapeutic potential of adult bone marrow-derived mesenchymal stem cells in diseases of the skeleton. *J Cell Biochem* 2010;111:249–257.
- Duijvestein M, Vos AC, Roelofs H et al. Autologous bone marrow-derived mesenchymal stromal cell treatment for refractory luminal Crohn's disease: Results of a phase I study. *Gut* 2010;59:1662–1669.
- Garcia-Olmo D, Herreros D, Pascual I et al. Expanded adipose-derived stem cells for the treatment of complex perianal fistula: A phase II clinical trial. *Dis Colon Rectum* 2009;52:79–86.
- Gao Z, Zhang Q, Han Y et al. Mesenchymal stromal cell-conditioned medium prevents radiation-induced small intestine injury in mice. *Cytotherapy* 2012;14:267–273.
- Aggarwal S, Pittenger MF. Human mesenchymal stem cells modulate allogeneic immune cell responses. *Blood* 2005;105:1815–1822.
- Kinnaird T, Stabile E, Burnett MS et al. Local delivery of marrow-derived stromal cells augments collateral perfusion through paracrine mechanisms. *Circulation* 2004;109:1543–1549.
- Brittan M, Chance V, Elia G et al. A regenerative role for bone marrow following experimental colitis: Contribution to neovasculogenesis and myofibroblasts. *Gastroenterology* 2005;128:1984–1995.
- Andoh A, Bamba S, Fujiyama Y et al. Colonic subepithelial myofibroblasts in mucosal inflammation and repair: Contribution of bone marrow derived stem cells to the gut regenerative response. *J Gastroenterol* 2005;40:1089–1099.
- Sémont A, Mouisseddine M, François A et al. Mesenchymal stem cells improve small intestinal integrity through regulation of endogenous epithelial cell homeostasis. *Cell Death Differ* 2010;17:952–961.
- Kudo K, Liu Y, Takahashi K et al. Transplantation of mesenchymal stem cells to prevent radiation-induced intestinal injury in mice. *J Radiat Res* 2010;51:73–79.
- Wachter S, Gerstner N, Goldner G et al. Endoscopic scoring of late rectal mucosal damage after conformal radiotherapy for prostatic carcinoma. *Radiat Oncol* 2000;54:11–19.
- Strup-Perrot C, Mathé D, Linard C et al. Global gene expression profiles reveal an increase in mRNA levels of collagens, MMPs, and TIMPs in late radiation enteritis. *Am J Physiol*

Gastrointest Liver Physiol 2004;287:G875–G885.

**20** Komori M, Tsuji S, Tsujii M et al. Involvement of bone marrow-derived cells in healing of experimental colitis in rats. *Wound Repair Regen* 2005;13:109–118.

**21** Bey E, Prat M, Duhamel P et al. Emerging therapy for improving wound repair of severe radiation burns using local bone marrow-derived stem cell administrations. *Wound Repair Regen* 2010;18:50–58.

**22** O'Brien PC. Radiation injury of the rectum. *Radiother Oncol* 2001;60:1–14.

**23** Fischer UM, Harting MT, Jimenez F et al. Pulmonary passage is a major obstacle for intravenous stem cell delivery: The pulmonary first-pass effect. *Stem Cells Dev* 2009;18:683–691.

**24** Rochefort GY, Vaudin P, Bonnet N et al. Influence of hypoxia on the domiciliation of mesenchymal stem cells after infusion into rats: Possibilities of targeting pulmonary artery remodeling via cells therapies? *Respir Res* 2005;6:125.

**25** François S, Bensidhoum M, Mouiseddine M et al. Local irradiation not only induces homing of human mesenchymal stem cells at exposed sites but promotes their widespread engraftment to multiple organs: A study of their quantitative distribution after irradiation damage. *STEM CELLS* 2006;24:1020–1029.

**26** Badylak SF, Valentin JE, Ravindra AK et al. Macrophage phenotype as a determinant of biologic scaffold remodeling. *Tissue Eng Part A* 2008;14:1835–1842.

**27** Griffin MD, Ritter T, Mahon BP. Immunological aspects of allogeneic mesenchymal stem cell therapies. *Hum Gene Ther* 2010;21:1641–1655.

**28** Németh K, Leelahavanichkul A, Yuen PS et al. Bone marrow stromal cells attenuate sepsis via prostaglandin E(2)-dependent reprogramming of host macrophages to increase their interleukin-10 production. *Nat Med* 2009;15:42–49.

**29** Cario E. Toll-like receptors in inflammatory bowel diseases: A decade later. *Inflamm Bowel Dis* 2010;16:1583–1597.

**30** Romieu-Mourez R, François M, Boivin MN et al. Cytokine modulation of TLR expression and activation in mesenchymal stromal cells leads to a proinflammatory phenotype. *J Immunol* 2009;182:7963–7973.

**31** Duffield JS, Forbes SJ, Constandinou CM et al. Selective depletion of macrophages reveals distinct, opposing roles during liver injury and repair. *J Clin Invest* 2005;115:56–65.

**32** Moodley Y, Atienza D, Manuelpillai U et al. Human umbilical cord mesenchymal stem cells reduce fibrosis of bleomycin-induced lung injury. *Am J Pathol* 2009;175:303–313.

**33** Taha Y, Raab Y, Larsson A et al. Vascular endothelial growth factor (VEGF): A possible mediator of inflammation and mucosal permeability in patients with collagenous colitis. *Dig Dis Sci* 2004;49:109–115.

**34** Chaudhary NI, Roth GJ, Hilberg F et al. Inhibition of PDGF, VEGF and FGF signalling attenuates fibrosis. *Eur Respir J* 2007;29:976–985.

**35** Wu Y, Chen L, Scott PG et al. Mesenchymal stem cells enhance wound healing through differentiation and angiogenesis. *STEM CELLS* 2007;25:2648–2659.

**36** Kanazawa S, Tsunoda T, Onuma E et al. VEGF, basic-FGF, and TGF-beta in Crohn's disease and ulcerative colitis: A novel mechanism of chronic intestinal inflammation. *Am J Gastroenterol* 2001;96:822–828.

**37** Abdollahi A, Li M, Ping G et al. Inhibition of platelet-derived growth factor signaling attenuates pulmonary fibrosis. *J Exp Med* 2005;201:925–935.

**38** Hetzel M, Bachem M, Anders D et al. Different effects of growth factors on proliferation and matrix production of normal and fibrotic human lung fibroblasts. *Lung* 2005;183:225–237.

**39** Lalu MM, McIntyre L, Pugliese C et al. Safety of cell therapy with mesenchymal stromal cells (SafeCell): A systematic review and meta-analysis of clinical trials. *Canadian Critical Care Trials Group. PLoS One* 2012;7:e47559.

**40** Rigotti G, Marchi A, Micciolo PR et al. On the safety of autologous fat grafting for breast reconstruction. *Plast Reconstr Surg* 2012;130:206e–207e.

**41** Voswinkel J, Francois S, Simon JM et al. Use of mesenchymal stem cells (MSC) in chronic inflammatory fistulizing and fibrotic diseases: A comprehensive review. *Clin Rev Allergy Immunol* 2013 [Epub ahead of print].



See [www.StemCellsTM.com](http://www.StemCellsTM.com) for supporting information available online.